Quantum effects in linear and non-linear transport of T-shaped ballistic junction

J. Wróbel,[1] P. Zagrajek,[1] M. Czapkiewicz,[1] M. Bek,[2] D. Sztenkiel,[1] K. Fronc,[1] R. Hey,[3] K. H. Ploog,[3] and B. R. Bułka[2]

[1]*Institute of Physics, Polish Academy of Sciences, al Lotników 32/46, 02-668 Warszawa, Poland*
[2]*Institute of Molecular Physics, Polish Academy of Sciences, ul. M. Smoluchowskiego 17, 60-179 Poznań, Poland*
[3]*Paul Drude Institute of Solid State Electronics, Hausvogteiplatz 5-7, D-10117 Berlin, Germany*

(Dated: December 10, 2009)

We report low-temperature transport measurements of three-terminal T-shaped device patterned from GaAs/$Al_xGa_{1-x}As$ heterostructure. We demonstrate the mode branching and bend resistance effects predicted by numerical modeling for linear conductance data. We show also that the backscattering at the junction area depends on the wave function parity. We find evidence that in a non-linear transport regime the voltage of floating electrode always *increases* as a function of *push-pull* polarization. Such anomalous effect occurs for the symmetric device, provided the applied voltage is less than the Fermi energy in equilibrium.

PACS numbers: 73.21.Nm, 73.23.Ad, 85.35.Ds

Recently, nanotechnology advances have led to a growing interest in electrical transport properties of the so-called three-terminal ballistic junctions (TBJs). As the name indicates, such structures consist of three quantum wires connected via a ballistic cavity to form a Y-shaped or T-shaped current splitter. One motivation is that in principle such systems can operate at high speed with a very low power consumption. Therefore, interesting and unexpected nonlinear transport characteristics of TBJs are intensively investigated due to possible applications as high frequency devices or logic circuits[1, 2].

Another reason for the increased number of studies devoted to TBJs are quantum mechanical aspects of carrier scattering, which dominate at low temperatures in the linear transport regime. This applies especially to T-shaped splitters. For example, it is expected that a T-branch switch, made of materials with a significant spin-orbit interactions, can act as an effective spin polarizer [3]. Also, for such geometry an ideal splitting of electrons from a Cooper pair is expected, provided the lower part of the letter T is made of a superconducting material [4]. Both effects rely very strongly on the perfect shape of the devices and high enough transparency of individual wires. Unfortunately, experimental data available for the lithographically perfect T-branch junctions are limited mostly to a non-linear transport regime [5]. Quantum linear transport is usually studied for less symmetric structures, typically consisting of short point contact attached to a side wall of a wider channel [6].

In this work we report on fabrication and low temperature transport measurements of T-shaped three-terminal devices, for which we take a special care to preserve the perfect symmetry and reduce the geometrical disorder. By comparing our data to conductance modeling by the recursive Green-function method, we find out that quantum effects dominate up to source-drain voltages equal to the Fermi energy. In particular, we show that the non-linear response of symmetric TBJ behaves in a non-classical way and is highly tunable with carrier density.

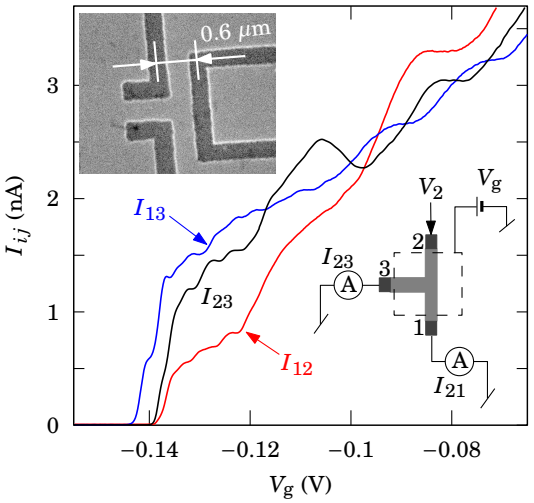

FIG. 1: (Color online) Currents I_{ij} vs gate voltage V_g at temperature $T \approx 0.3$ K. I_{ij} is defined as current flowing from contact j when voltage V_i is applied to terminal i (see the measurement scheme). Upper inset shows scanning electron micrograph of the T-junction device, top metal gate is not visible here.

The three-terminal ballistic junctions are made of a GaAs/AlGaAs:Si heterostructure with electron concentration $n_{2D} = 2.3 \times 10^{11}$ cm^{-2} and carrier mobility $\mu = 1.8 \times 10^6$ cm^2/Vs. The interconnected wires of equal length $L = 0.6$ μm and lithographic width $W_{\rm lith} = 0.4$ μm are patterned by e-beam lithography and shallow-etching techniques to form a T-shaped nanojunction (see inset to Fig.1). The physical width of all branches is simultaneously controlled by means of a top metal gate which is evaporated over the entire structure. The differential conductances have been measured in a He-3/He-4 dilution refrigerator, by employing a standard low-frequency lock-in technique. We have also studied non-linear transport in the typical for TBJs, so-called *push-pull* bias

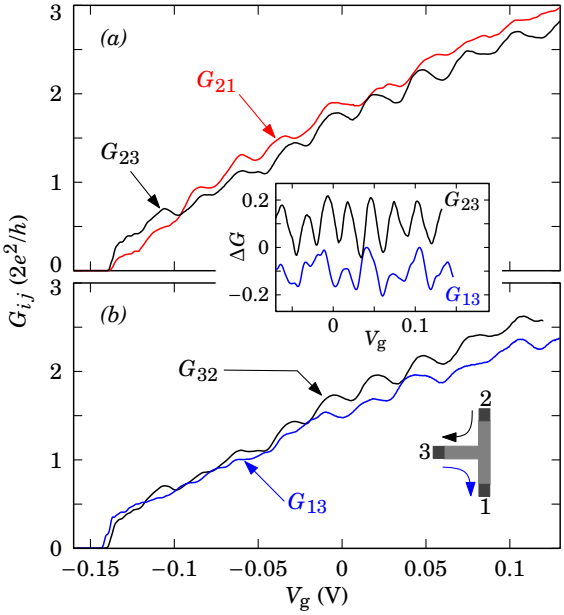

FIG. 2: (Color online) $G_{ij} = I_{ij}/V_i$ plotted vs gate voltage at $T \approx 0.3$ K. (a) G_{23} and G_{21}. (b) G_{32} and G_{13}, here both conductances involve transmission to side terminal 3. Inset: comparison between G_{23} and G_{13} oscillations, a smooth backgrounds have been removed from the original data (ΔG is in $2e^2/h$ units, V_g is in volts).

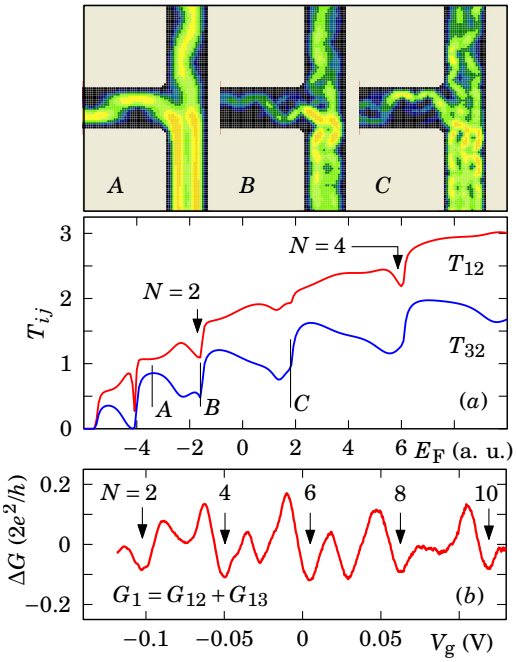

FIG. 3: (Color online) (a) Local current intensity (upper panel) and transmission coefficients T_{ij} vs Fermi energy E_F (below). Lines A, B and C mark energy values for which the local current densities have been calculated. Black color in density plot corresponds to zero current and bright areas to maximal current intensity. (b) Conductance $G_1 = G_{12} + G_{13}$ vs gate voltage, $T \approx 0.3$ K. Only oscillating part is shown, a smooth background has been removed. Arrows on both subfigures indicate backscattering at even mode numbers.

regime, when equal but opposite in sign *dc* voltages are simultaneously applied to the opposite input contacts.

The application of a metal gate over the active region of the device helps to symmetrize transmission coefficients by smoothing the confinement potential [7]. Nevertheless, even a perfectly shaped and gated junction may remain disordered at low electron densities, when screening effects are weak. Figure 1 shows linear currents flowing from each of three terminals for negative gate voltages close to the threshold regime. The data indicate clearly that there is a weak asymmetry between contacts – channels open at slightly different V_g. Additionally, small reproducible wiggles are visible above threshold voltage. All investigated structures show similar behavior and we attribute it to the presence of *quasi*-localized states, formed in the central part of the device. In this paper we present data for the sample which has a lowest disorder and highest degree of symmetry.

Although channel $2 \to 1$ opens last, at higher electron densities I_{12} is larger than I_{23} and I_{13}, as predicted by Baranger [8] for the ideal T-shaped quantum splitter. Figure 2 presents the conductances G_{ij} as a function of gate voltage up to +0.12 V. For $V_g > -0.05$ V the regular oscillations corresponding to the successive population of electric sub-bands in each of the three terminals are visible. Since magnetic field is zero, we expect $G_{ij} = G_{ji}$ and this is indeed observed in the experiment. For example, curves G_{23} and G_{32} are almost identical. Larger differences are noticed for G_{13} and G_{23} curves which should be equal for the perfectly shaped device. Relevant data are presented in the inset to Fig.2 where oscillating parts of G_{23} and G_{13} are compared. On average G_{13} is smaller and oscillate less regularly than G_{23}. Nevertheless, maxima and minima on both curves are close to each other and for $V_g > 0.05$ V they oscillate exactly in phase. It means that starting from a disordered structure at the threshold voltage, for $V_g \gtrsim 0$ the device becomes more symmetrical and experimental data can be compared with the theory of ballistic transport.

We model TBJ by three semi-infinite strips of "atoms" and the square coupling region. Calculations have been performed at temperature $T = 0$, using a tight-binding approach and a recursive Green functions technique [9]. To determine a local current intensity inside the junction we have incorporated parts of each wire to the coupling region and used a newly developed, so-called knitting algorithm [10]. Results of this modeling are presented in Fig. 3(a). Transmission coefficients T_{ij} between j-th and i-th electrode are calculated for disorder free and symmetric device with *rounded corners* in the coupling region. Note that the value of T_{21} increases almost monotonically as a function of energy, whereas T_{32} oscillates strongly. This is the co-called *bend resistance effect*. T_{32}

reaches maximum when the upper, just populated subband, is almost fully transmitted to the terminal 3 (see intensity plot A). For higher kinetic energies, however, coupling becomes weaker and as a result T_{32} decreases, leading to the non-monotonic behavior as a function of Fermi energy E_F.

Presented calculations are consistent with the experimental data obtained at electron densities high enough. For $V_g > 0$ the curve G_{21} is similar to T_{21} and rather smooth as compared to G_{23}, which (like T_{23}) shows deeper minima due to the bend resistance effect (see Fig. 2). Note also, that calculated energy dependence of transmission coefficients differ for odd and even channel numbers. For example, the backscattering for $N = 2$ and $N = 4$ channels is stronger, as indicated with arrows in Fig. 3. This effect was already predicted for a perfect T coupler [8] and is apparently enhanced by the rounding of the "corners" in a junction area. For even parity modes electron has high probability density at the center of the device and therefore is more likely transmitted (to see this compare density plots B and C). We believe that such conductance dependence on wave function parity is also observed in the experiment. It is especially well resolved for the total conductance $G_1 = I_1/V_1 = G_{12}+G_{13}$. Relevant data are presented in Fig. 3(b).

Next we consider the measurement scheme where stub terminal (3) acts as a floating voltage probe ($I_3 = 0$). For a classical device we have $V_3 = (V_1 - V_2)/2$. This simple formula should be modified for ballistic transport, where it takes form $V_3/V_1 = T_{31}/(T_{31} + T_{32})$ with $V_2 = 0$ for simplicity. If $T_{31} = T_{32}$ then classical result $V_3/V_1 = 1/2$ is recovered.

Conductance data shown in Fig. 2(b) indicate that on average G_{31} is smaller than G_{32}. Therefore, to imitate the real sample, we rounded the junction "corners" of a model device in such a way that $T_{31} < T_{32}$. The shape of the coupling area and results of calculations are shown in Fig. 4(a). Ratio V_3/V_1 is on average below 1/2 but oscillates as energy increases. Very similar dependence is observed in the experiment. The measured value of V_3/V_1 ratio reaches maximum, each time a new one-dimensional level becomes occupied. Interestingly, theory also predicts the occurrence of additional asymmetric and very narrow resonances when a new conduction channel opens to transport in stub terminal. They are probably related to the so-called Wigner singularities, which exist when the energies of quantized levels in a side probe differ from those in the rest of the device[9]. Similar features are also visible in the experiment, especially for $-0.1 < V_g < 0$, but their possible connection to Wigner resonances requires further studies.

Now let us turn to the non-linear transport regime where the probabilities of transmission from input terminals to a floating contact may differ, even for a perfect device. In such case, when V_1 is large enough and positive, then V_3/V_1 is *less* then 1/2. Equivalently, if $V_1 = V_{pp}$ and $V_2 = -V_{pp}$ (*push-pull* bias regime) then $V_3 = V_C$ is *always negative*, as it was predicted in [11] and then proved experimentally [12]. Using the quantum scattering approach Csontos and Xu [13] extended the calculation range to a low temperature regime. They showed that V_C may be also *positive*, provided $\partial T_{31}/\partial E_F = \partial T_{32}/\partial E_F < 0$ and $kT \ll E_F$. To our knowledge, however, the predictions of Ref. [13] have not been confirmed experimentally.

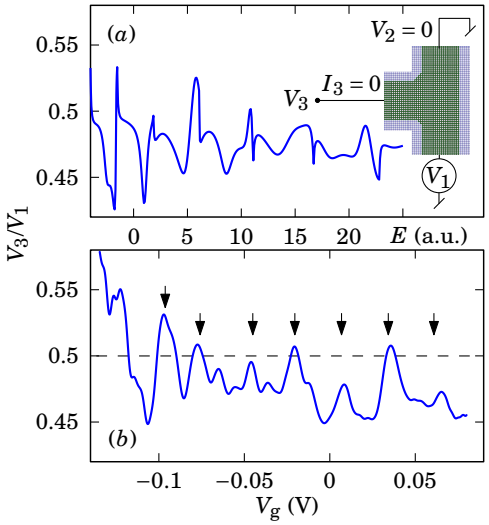

FIG. 4: (Color online) (a) V_3/V_1 ratio vs energy, calculated for a device with asymmetrically rounded corners in the coupling region (see inset). (b) V_3/V_1 data obtained as a function of gate voltage at $T \approx 0.2$ K for $V_1 = 50$ μV (measurement scheme is shown above). Arrows correspond to minima on G_{23} curve.

Figure 5(a) shows measurement schematics and corresponding V_C data obtained when $|V_{pp}| < 15$ mV. V_C is not a symmetric function of V_{pp}, yet above a certain threshold, data — as expected — bend towards negative values of V_C. Such behavior is often observed in experiments [12] because $T_{31} \neq T_{32}$ due to imperfections which are always present in the real devices. Apart from such asymmetry, however, data reported here behave in an *anomalous* way. When a linear trend has been removed, V_C first *increases* with $|V_{pp}|$, and then goes down reaching maximum at ~ 7 mV. To investigate this effect in more detail we have used a modulation method to measure the *switching parameter* $\beta = \partial V_C/\partial V_{pp}$ directly with a better voltage resolution. Figure 5(a) explains the measurement idea and Fig. 5(b) shows values of parameter $\beta_s = \beta - \beta_a$ as a function of V_{pp} for a different gate voltages. Here β_a is the mean value of switching parameter calculated at each V_g for $|V_{pp}| < 15$ mV. Subtracting β_a is equivalent to removing a linear trend from the *dc* data and therefore reduces the influence of the T_{31} vs T_{32} asymmetry.

To compare the experimental findings with theory we

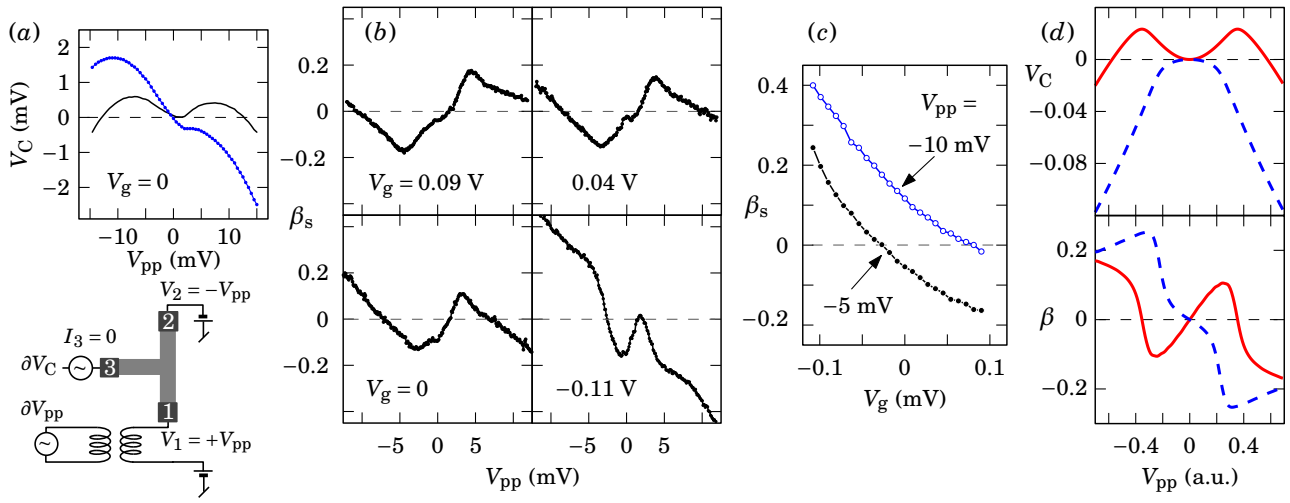

FIG. 5: (Color online) (a) Stub voltage V_C vs push-pull polarization V_{pp} at $V_g = 0$ (dotted line). The same data with a linear trend removed are also shown (solid line). Below: experimental setup; small *ac* voltage (50 μV) is inductively coupled to V_{pp} , $\beta = \partial V_C/\partial V_{pp}$ is measured directly using a low-frequency lock-in technique. (b) Variation in $\beta_s = \beta - \beta_a$ with the applied V_{pp} for V_g of 0.09 , 0.04, 0 and −0.11 V; here β_a is the mean value of β and equals −0.18, −0.15, −0.12, and 0.01 respectively. (c) Variation in β_s with gate voltage for V_{pp} of −10 and −5 mV. All experimental results at $T = 0.8$ K. (d) Nonlinear transport data calculated for an ideal T-shaped junction. Solid line: $E_F = -1.55$, $\partial T_{31}/\partial E_F < 0$. Dashed line: $E_F = -1.15$, $\partial T_{31}/\partial E_F > 0$. E_F, V_C and V_{pp} in arbitrary units.

calculated V_C and β for an ideal T-shaped junction from the energy dependence of a transmission coefficients. Results are consistent with the explanation of Xu [11], as it follows from Fig. 5(d). If $\partial T_{31}/\partial E_F < 0$ then V_C *increases* with $|V_{pp}|$ and β has a positive slope in this voltage range. When $\partial T_{31}/\partial E_F > 0$ stub voltage is negative and switching parameter behaves "normally". Interestingly, when experimental V_C data are compared to linear conductance $G_3 = G_{31} + G_{32}$, *no* such correlation can be found. For example at $V_g = 0$, 0.04, and 0.09 V, derivative $\partial G_3/\partial V_g$ is negative, positive and approximately zero, but switching parameter does not change its shape and sign as would be expected from modeling. Results indicate that an anomalous data range, where β has a positive slope, always exists — only its width decreases with E_F. This fact can be used to tune switching parameter with the gate voltage. Figure 5(c) shows β_s as a function of V_g for the two values of V_{pp}. Remarkably, not only amplitude but also the *sign* of β_s can be changed. We conclude that the behavior of V_C in Fig. 5 cannot be explained by a single particle transmission approach. Probably, as suggested in [14], the non-linear transport regime requires a self-consistent calculations.

In summary, we have shown that linear transport in T-shaped ballistic junction can be successfully described by quantum scattering effects and weak disorder in a cavity area. We have shown for the first time, that stub voltage can *increase* as a function of *push-pull* polarization in a non-linear transport regime, however, the energy dependence of such non-equilibrium effect is inconsistent with the standard single-particle picture of electron transmission. Nevertheless, novel applications of symmetric TBJ structure, for example as the component of a multilogic device, are still possible.

This work was funded by grant No. 107/ESF/2006 and MNiSW projects N202/103936 and N202/229437.

[1] H. Q. Xu, Nat. Mater. **4**, 649 (2005).
[2] L. Worschech, D. Hartmann, S. Reitzenstein, and A. Forchel, in J. Phys.: Condens. Matter **17**, R775 (2005).
[3] A. A. Kiselev and K. W. Kim, Appl. Phys. Lett. **78**, 775 (2001).
[4] A. Bednorz, J. Tworzydło, J. Wróbel, and T. Dietl, Phys. Rev. B **79**, 245408 (2009).
[5] D. Wallin, I. Shorubalko, H. Q. Xu, and A. Cappy, Appl. Phys. Lett. **89**, 092124 (2006); D. Spanheimer, C. R. Muller, J. Heinrich, S. Hofling, L. Worschech, and A. Forchel, Appl. Phys. Lett. **95**, 103502 (2009).
[6] T. Usuki, M. Saito, M. Takatsu, R. A. Kiehl, and N. Yokoyama, Phys. Rev. B **52**, 8244 (1995); A. Ramamoorthy, J. P. Bird, and J. L. Reno, J. Phys.: Condens. Matter **19**, 276205 (2007).
[7] J. Liu, W. X. Gao, K. Ismail, K. Y. Lee, J. M. Hong, and S. Washburn, Phys. Rev. B **50**, 17383 (1994).
[8] H. U. Baranger, Phys. Rev. B **42**, 11479 (1990).
[9] B. R. Bułka and A. Tagliacozzo, Phys. Rev. B **79**, 075436 (2009), and references therein.
[10] K. Kazymyrenko and X. Waintal, Phys. Rev. B **77**, 115119 (2008).
[11] H. Q. Xu, Applied Physics Letters **78**, 2064 (2001).
[12] I. Shorubalko, H. Q. Xu, I. Maximov, P. Omling, L. Samuelson, and W. Seifert, Applied Physics Letters

79, 1384 (2001); L. Worschech, H. Q. Xu, A. Forchel, and L. Samuelson, Appl. Phys. Lett. **79**, 3287 (2001).

[13] D. Csontos and H. Q. Xu, Phys. Rev. B **67**, 235322 (2003).

[14] M. Büttiker and D. Sánchez, Phys. Rev. Lett. **90**, 119701 (2003).